






Dissecting the labdane-related diterpenoid biosynthetic gene clusters in rice reveals directional cross-cluster phytotoxicity

Riqing Li^{1*} , Juan Zhang^{2*} , Zhaohu Li^{3,4} , Reuben J. Peters²  and Bing Yang^{1,5} 

¹Division of Plant Sciences, Bond Life Sciences Center, University of Missouri, Columbia, MO 65211, USA; ²Roy J. Carver Department of Biochemistry, Biophysics and Molecular Biology, Iowa State University, Ames, IA 50011, USA; ³State Key Laboratory of Physiology and Biochemistry, College of Agronomy and Biotechnology, China Agricultural University, Beijing 100193, China; ⁴College of Plant Science and Technology, Huazhong Agricultural University, Wuhan 430070, China; ⁵Donald Danforth Plant Science Center, St Louis, MO 63132, USA

Summary

Authors for correspondence:

Zhaohu Li

Email: lizhaohu@cau.edu.cn

Reuben J. Peters

Email: rjpeters@iastate.edu

Bing Yang

Email: yangbi@missouri.edu

Received: 15 May 2021

Accepted: 12 October 2021

New Phytologist (2022) **233**: 878–889

doi: 10.1111/nph.17806

Key words: CRISPR, disease resistance, diterpenoid, gene cluster, phytoalexin, rice.

- Rice (*Oryza sativa*) is a staple food crop and serves as a model cereal plant. It contains two biosynthetic gene clusters (BGCs) for the production of labdane-related diterpenoids (LRDs), which serve important roles in combating biotic and abiotic stress. While plant BGCs have been subject to genetic analyses, these analyses have been largely confined to the investigation of single genes.
- CRISPR/Cas9-mediated genome editing was used to precisely remove each of these BGCs, as well as simultaneously knock out both BGCs.
- Deletion of the BGC from chromosome 2 (c2BGC), which is associated with phytocassane biosynthesis, but not that from chromosome 4 (c4BGC), which is associated with momilactone biosynthesis, led to a lesion mimic phenotype. This phenotype is dependent on two closely related genes encoding cytochrome P450 (CYP) mono-oxygenases, *CYP76M7* and *CYP76M8*, from the c2BGC. However, rather than being redundant, *CYP76M7* has been associated with the production of phytocassanes, whereas *CYP76M8* is associated with momilactone biosynthesis. Intriguingly, the lesion mimic phenotype is not present in a line with both BGCs deleted.
- These results reveal directional cross-cluster phytotoxicity, presumably arising from the accumulation of LRD intermediates dependent on the c4BGC in the absence of *CYP76M7* and *CYP76M8*, further highlighting their interdependent evolution and the selective pressures driving BGC assembly.

Introduction

As the staple food for over half of the global population, rice is a critically important crop (Muthayya *et al.*, 2014). In addition, rice serves as a model cereal plant due, in no small part, to the small size of its genome, which led to early sequencing (Goff *et al.*, 2002; Yu *et al.*, 2002). Among the early findings from the rice genome sequence was the presence of two biosynthetic gene clusters (BGCs), associated with the production of antimicrobial phytoalexins, which were among the first defence proteins to be reported (Nutzmann *et al.*, 2016). More specifically, these clusters contained genes encoding enzymes for biosynthesis of labdane-related diterpenoids (LRDs), which have long been postulated to serve as phytoalexins and allelochemicals in rice (Peters, 2006), with recent results demonstrating roles in resistance to abiotic as well as biotic stress (Lu *et al.*, 2018; Zhang *et al.*, 2021). Indeed, LRDs are now known to serve such roles in cereal crops more generally (Murphy & Zerbe, 2020), further emphasising their importance.

*These authors contributed equally to this work.

The LRDs are characterised by initial bicyclisation of the general diterpenoid precursor (*E,E,E*)-geranylgeranyl diphosphate (GGPP) catalysed by class II diterpene cyclases (Peters, 2010). These cyclases most often produce the eponymous labdadienyl/copalyl diphosphate (CPP), leading to the designation of the relevant enzymes as CPP synthases (CPSs). CPP can be produced in different stereochemical configurations, with the production of *ent*-CPP required in all vascular plants (tracheophytes) for gibberellin (GA) phytohormone biosynthesis (Zi *et al.*, 2014). Rice also produces *syn*-CPP and LRD phytoalexins derived from this, but also from *ent*-CPP (Peters, 2006). Further cyclisation and/or rearrangement of CPP is catalysed by class I diterpene synthases, again with all tracheophytes necessarily containing an *ent*-kaurene synthase (KS) for GA biosynthesis, which has given rise to evolutionarily derived enzymes termed KS-like (KSL) (Zi *et al.*, 2014).

The rice genome was found to contain two BGCs, defined as proximal unrelated genes involved in a common biosynthetic pathway, for LRDs, with one on chromosome (chr.) 2 (c2BGC), and the other on chr. 4 (c4BGC) (Schmelz *et al.*, 2014). These BGCs contain not only sequentially acting CPSs and KSLs, but

also cytochrome P450 (CYP) mono-oxygenases as well as, for the c4BGC, short chain alcohol dehydrogenases (Fig. 1). Notably, the c4BGC is clearly associated with momilactone biosynthesis, while c2BGC is largely associated with phytocassane biosynthesis, representing the two most prevalent LRDs produced by rice (Yamane, 2013), although c2BGC also clearly contains both KSLs and CYPs involved in additional LRD metabolism (Swaminathan *et al.*, 2009; Wu *et al.*, 2011).

The occurrence of BGCs, proximal unrelated genes involved in a common biosynthetic pathway, is somewhat unusual in eukaryotic genomes (Nutzmann *et al.*, 2018). These seem to be associated with the production of secondary metabolites not required for normal growth and development. However, not all such biosynthetic pathways are associated with BGCs, leaving the evolutionary pressures underlying their assembly in question. This has been suggested to arise from a combination of positive and negative selection pressures, both for production of bioactive metabolites but also against the accumulation of certain intermediates (Swaminathan *et al.*, 2009; Takos & Rook, 2012). Indeed, investigation of the rice c4BGC provided the first evidence for such negative effects from incomplete pathway inheritance, as a

T-DNA insertion knock-out mutant of *OsKSL4* was found to exhibit significantly reduced seed germination rates (Xu *et al.*, 2012). Notably, this study also utilised a T-DNA insertion knock-out mutant of *OsCPS4*, but found that the momilactones seemed to primarily act as allelochemicals rather than in defence against the fungal blast pathogen *Magnaporthe oryzae* (Xu *et al.*, 2012), at least in the relevant cultivar (cv) Zhonghua 11, despite the fact that these were the first phytoalexins against *M. oryzae* found in rice (Cartwright *et al.*, 1981). Conversely, a T-DNA insertion knock-down mutant of *OsCPS4* found in a different rice cv (Nipponbare) did effect resistance to *M. oryzae* as well as allelopathic activity (Toyomasu *et al.*, 2014).

Other genetic studies have been directed at these rice BGCs, albeit also primarily targeted at single genes or at a pair of closely related paralogues to investigate the role of the encoded enzyme (s) in LRD biosynthesis, and occasionally that of the resulting LRDs in microbial disease resistance, rather than probing BGC evolution *per se*. For example, consistent with their localisation within the c4BGC, RNA-interference (RNAi)-mediated knock-down of the closely related *CYP99A2* and *CYP99A3* provided the first evidence that these play a role in momilactone

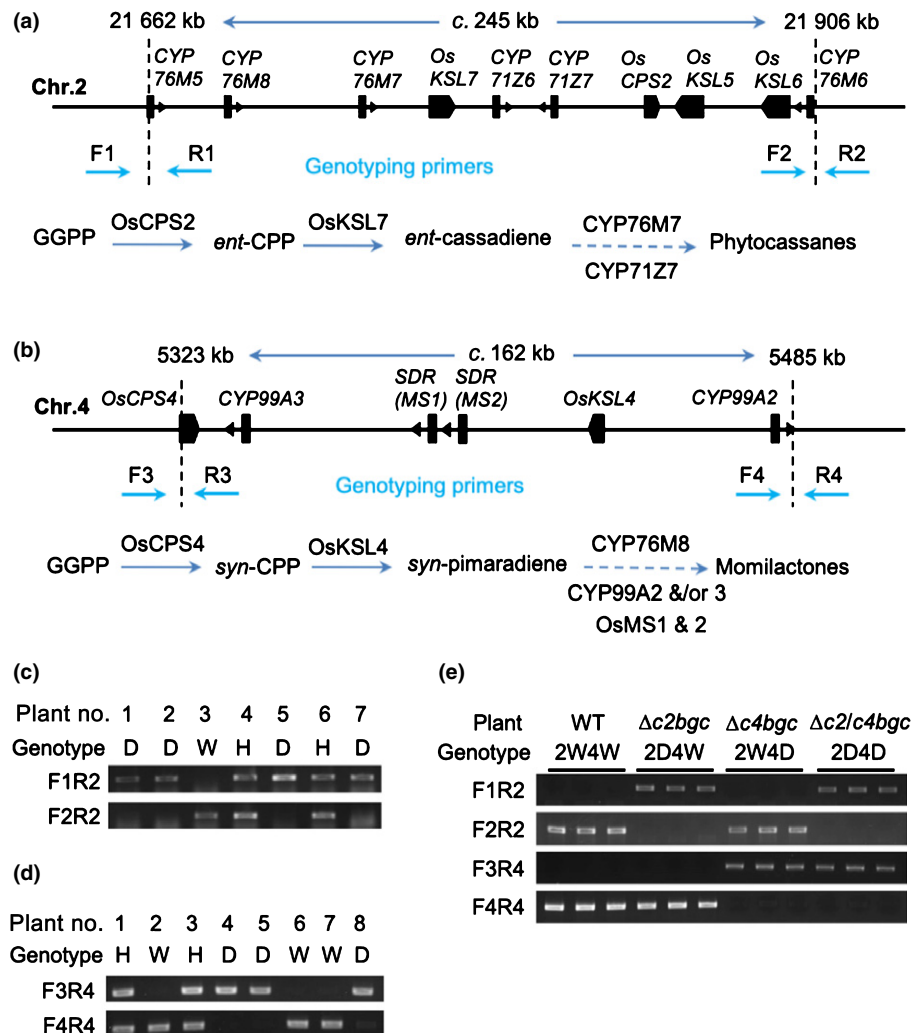


Fig. 1 Large deletions of the rice diterpenoid biosynthetic gene clusters (BGCs). (a, b) Gene structure of diterpenoid on chromosomes 2 (a) and 4 (b), and associated biosynthesis pathways. The filled boxes represent genes. Dashed vertical lines represent locations of genomic break sites. Dashed arrows indicate multiple enzymatic reactions leading to production of diterpenoid families (known steps shown in Supporting Information Fig. S1). (c–e) Genotyping of progeny rice plants derived from the fragmental deletion mutants and their crossing using deletion-specific primers. The numbers 2 and 4 in front of genotype represent chr.2 and chr.4, respectively. CPS, copalyl diphosphate synthase; CYP, cytochrome P450; Genotype D, mutant homozygous for deletion; GGPP, geranylgeranyl diphosphate; H, Heterozygous; KSL, *ent*-kaurene synthase-like; SDR, short-chain alcohol dehydrogenase/reductase; W, WT.

biosynthesis (Shimura *et al.*, 2007). Similarly, consistent with their localisation within the c2BGC, RNAi knock-down of the closely related *CYP76M7* and *CYP76M8* was used to indicate that these play a role in phytocassane biosynthesis (Wang *et al.*, 2012). Correlation of the c2BGC with phytocassane production was further bolstered by the finding that a T-DNA insertion knock-out mutant of the similarly c2BGC localised *CYP71Z7* was deficient in a certain transformation (hydroxylation at carbon-2) in the underlying metabolic network (Ye *et al.*, 2018). Finally, the potential redundancy of *ent*-CPP-derived LRD metabolism in rice was investigated using a T-DNA insertion knock-out mutant of *OsCPS2*, revealing that this is insufficient to completely block production of the phytocassanes or other *ent*-CPP-derived LRDs, presumably due to the presence of *OsCPS1* required for GA phytohormone biosynthesis, which enables continued production of *ent*-CPP (Lu *et al.*, 2018). This study also further investigated the role of rice LRDs in microbial disease resistance, including the use of the *OsCPS4* T-DNA insertion knock-out mutant, which uncovered a role for *syn*-CPP-derived (*OsCPS4*-dependent) LRDs in nonhost disease resistance to *Magnaporthe poae*, as well as roles for *OsCPS2*-associated (*ent*-CPP-derived) LRDs in defence against bacterial leaf blight pathogen *Xanthomonas oryzae* pathovar (pv) *oryzae* (*Xoo*) as well as *M. oryzae* (Lu *et al.*, 2018).

Development of the CRISPR/Cas9 technique has offered precise genome editing that has now been applied to rice (Char *et al.*, 2019), and even more specifically to its LRD BGCs in work targeted at the fast-growing cv Kitaake. In particular, this approach is most often applied to target single genes and has been used in this context to provide a direct comparison of knocking-out *OsCPS2* and/or *OsCPS4* in the same genetic background, with crossing of the initially generated *cps2* and *cps4* single-mutant lines to generate a *cps2x4* double-mutant line (Zhang *et al.*, 2021). Similarly, the closely related *CYP76M7* and *CYP76M8* also have been individually knocked out, revealing that *CYP76M7* is primarily associated with phytocassane biosynthesis, while *CYP76M8* is more important for momilactone production, although these do appear to be partially redundant (Kitaoka *et al.*, 2021). However, the co-localisation of these two genes in the c2BGC essentially blocks the production of a double-mutant line by genetic crossing. Fortunately, CRISPR/Cas9 can be applied to simultaneously target multiple genes/loci (Bi & Yang, 2017), enabling the investigation of neighbouring genes such as those found in BGCs, or even removal of large fragments such as entire BGCs (Li *et al.*, 2019). Indeed, deletion of the rice LRD BGCs using CRISPR/Cas9 has previously been reported in protoplasts and, for deletion of the c2BGC, in T0 plants, although this was only present in mono-allelic form with the c. 245 kb deletion paired with small nucleotide changes at the targeted sites in the other copy of the c2BGC (Zhou *et al.*, 2014).

Here we report that deletion of the c2BGC, as well as the c4BGC, yields lines that are viable and genetically stable in the homozygous form. This enabled a chemotypic and phenotypic investigation of such complete BGC loss, revealing not only the expected effects on rice LRD metabolism and microbial disease

resistance, but also the discovery of a lesion mimic phenotype for homozygous c2BGC deletion plants. CRISPR/Cas9 multiplex targeting was then used to demonstrate that the lesion mimic phenotype depends on both *CYP76M7* and *CYP76M8*, as exhibited by *cyp76m7/8* double, but not *cyp76m7* or *cyp76m8* single, mutant lines. Intriguingly, it was further possible to cross the BGC deletion lines to create a viable line missing both BGCs, which no longer exhibited the lesion mimic phenotype. This indicates that the lesions arise from directional phytotoxicity, presumably from c4BGC-dependent LRD intermediates that accumulate in the absence of the c2BGC, specifically loss of *CYP76M7* and *CYP76M8*.

Materials and Methods

Plant materials and growth conditions

The *japonica* cultivar (*Oryza sativa*) Kitaake was used here. The T0 plants with each BGC deleted had been generated previously using CRISPR/Cas9 genome editing (Zhou *et al.*, 2014; Li *et al.*, 2019). Rice seeds were sterilised in 2% sodium hypochlorite and grown aseptically on half-strength Murashige & Skoog (½MS) medium containing 3% sucrose and 0.5% agar (pH 5.8) in plastic container at 30°C. Here, 2-wk-old seedlings were transferred and planted to large plastic boxes containing farm soil and grown in a glasshouse (unless alternatively indicated). Growth conditions were 30°C in daytime, 28°C in nighttime, and with a 13-h day length.

Phytochemical analyses

The 3-wk-old rice leaves were cut into 5-cm pieces and 0.1 g was induced by floating on a solution of 0.5 mM CuCl₂. After 72 h these induced leaves were frozen by submersion into liquid N₂ and ground into a fine powder, then were extracted by shaking in 3 ml methanol for 72 h in a cold (4°C) room. Each sample had 2.31 µg sclareol added as an internal standard, and filtered through a 0.2-µm nylon filter (F2513-2; Thermo Fisher Scientific, Waltham, MA, USA) using a glass syringe, dried under a stream of N₂ gas, and resuspended in 1 ml methanol for analysis.

Analyses were carried out via liquid chromatography tandem mass spectrometry (LC-MS/MS), with 15-µl samples injected onto a Supelco (Sigma-Aldrich) Ascentis C18 column (10 cm × 2.1 mm; 3 µm) using an Agilent Technologies 1100 Series high performance liquid chromatography system coupled to both an ultraviolet-visible (UV-Vis) light diode array detector and an Agilent Technologies Mass Selective Trap SL detector located in the Iowa State University W.M. Keck Metabolomics Research Laboratory. A binary gradient was used, consisting of water with 0.1% acetic acid v/v (buffer A) and acetonitrile with 0.1% acetic acid v/v (buffer B). The solvent gradient elution was programmed as follows: initial, 40% buffer B; 0–13 min, a linear gradient from 40% buffer B to 85% buffer B; 13–14 min, a linear gradient from 85% buffer B to 100% buffer B; 14–14.5 min, a linear gradient from 100% buffer B to 40% buffer B. The known rice LRD phytoalexins were detected by MS/MS analysis, using an

isolation selection window of ± 0.5 m/z . The isolated masses were re-ionised and the resulting mass spectra recorded.

The isolated parent ions and quantified secondary ions, along with the corresponding retention time (RT), based on optimisation with the available authentic standards, for the known rice LRD phytoalexins were as follows: momilactone A, m/z 315.2–271.2, RT 11.1 min; momilactone B, m/z 331.2–269.2, RT 9.0 min; oryzalexin A, m/z 303.2–285.2, RT 10.0 min; oryzalexin B, m/z 303.3–286.2, RT 9.7 min; oryzalexin C, m/z 301.2–283.2, RT 9.6 min; oryzalexin D, m/z 287.2–269.2 (147.2), RT 9.6 min; oryzalexin E, m/z 287.2–269.2, RT 11.3 min; oryzalexin S, m/z 287.2–269.2 (241.2), RT 9.7 min; phytocassane A, m/z 317.2–299.2, RT 7.6 min; phytocassane B, m/z 335.2–317.2, RT 7.3 min; phytocassane C, m/z 319.2–301.2, RT 6.8 min; phytocassane D, m/z 317.2–299.2, RT 9.7 min; phytocassane E, m/z 317.2–299.2, RT 8.3 min; phytocassane F, m/z 333.2–315.2, RT 7.3 min; sclareol, m/z 273.2–163.1, RT 13.6 min. The relative amount of each LRD was determined with the 6300 Series Ion Trap LC/MS v.1.8 software package (Thermo Fisher Scientific), by comparison of total ion peak areas to that of the sclareol internal standard.

Fungal resistance assays

Magnaporthe oryzae strains CA89 and O254 were used, and infection assays were performed as previously described (Sesma & Osbourn, 2004). Briefly, rice seedlings at the third leaf stage were used for infection. Four pots of 20 plants were used per line and per experiment. Each pot was sprayed with 5 ml of a suspension of 10^5 conidia per millilitre. The sprayed plants were then incubated in the growth chamber with humid conditions (85% relative humidity, 25°C, and a 16 h : 8 h, light : dark photoperiod) for 6 d to score disease symptoms. Leaf lesions were scanned and analysed with ASSESS 2.0 software (American Phytopathological Society). Blast lesions were evaluated based on lesion number and lesion extension of disease symptoms as previously reported (Tucker *et al.*, 2010). One-way ANOVA statistical analyses were performed to compare wild-type and $\Delta c2bgc$ and $\Delta c4bgc$ plants. The Dunnett's significant difference test was used for post-ANOVA pairwise analysis of significance, set at 5% ($P < 0.05$).

Bacterial resistance assays

Xanthomonas oryzae pv *oryzae* (*Xoo*) strain PXO99^A and its *hrpC*, a gene encoding a type III secretion system, mutant PXO99^AME7 (ME7, for short) were used for leaf blight disease assays. *Xoo* was grown for 2–3 d on TSA (1% (w/v) tryptone, 1% sucrose, 0.1% glutamic acid, and 1.5% agar, pH 6.8) plates at 28°C, scraped off and resuspended in sterile deionised water. The suspension was then adjusted to an optical density of 0.5 at 600 nm before infection. Here, 2-wk-old seedlings were inoculated using a needleless syringe infiltration method (Zhu *et al.*, 1998), with five infiltrated spots on each leaf. The leaves were then harvested 2 d after injecting and ground sufficiently in a sterile mortar by adding a specified volume of sterile water. The subsequent solution was serially diluted and spread on TSA plates

to count colonies, then converted into colony formation units per infiltration spot. Bacterial counting was performed three times in parallel for each rice line. One-way ANOVA statistical analyses were applied to compare wild-type and $\Delta c2bgc$ and $\Delta c4bgc$ plants after bacterial inoculation. Dunnett's significant difference test was used for post-ANOVA pairwise analysis of significance, set at 5% ($P < 0.05$) (Fig. 4a–c; as described later).

Next, 8-wk-old rice plants were inoculated using the leaf-tip-clipping method (Kauffman *et al.*, 1973). Symptoms were scored by measuring lesion lengths after 14 d for the leaf-clipping inoculations. Lesion length measurements are the averages of 20 leaves. Lesion length of $\Delta c2bgc$ mutant plants was compared with wild-type (WT) plants after PXO99^A inoculation. ***, $P < 0.001$, calculated using post-ANOVA pairwise analysis of significance with the Dunnett's test (Fig. 5g; as described later).

For *in vitro* antimicrobial activity assays, 150 germinated seeds from each rice line were grown in a sterile beaker with 10 ml of ½MS medium for 15 d in 30°C growth chamber. The liquid solution containing root exudates from each line was collected separately. Liquid TSA medium containing 50% (v/v) of the root exudates was used for *Xoo* culture. The initial *Xoo* suspension was adjusted to an optical density (OD) of 0.15 at 600 nm and then grown with shaking in a 30°C incubator. OD₆₀₀ values were collected at the specified time points for the growth curves for bacteria.

3,3'-Diaminobenzidine staining

For measurement of H₂O₂ accumulation, leaves were collected at 45 d after germination and immediately submerged in a solution containing 1 mg ml⁻¹ DAB, and then incubated at room temperature in the dark for 8 h. The stained leaves were then decoloured in 95% boiling ethanol for 10 min and soaked for 2 d in 95% ethanol until all chlorophyll had been removed.

RNA isolation and gene expression analysis

Total RNA was extracted using TRIzol reagent (Thermo Fisher Scientific) according to the manufacturer's instructions. First-strand cDNA synthesis for RT-PCR was carried out using iScriptTM cDNA Synthesis kit (Bio-Rad) and random primers. A real-time PCR reaction was conducted in the CFX96 Touch Real-Time PCR Detection System (Bio-Rad) using SYBR Green Supermix (Bio-Rad) according to the manufacturer's instructions. The primer pairs used to specifically amplify target genes and *Actin1* are listed in Supporting Information Table S3.

Genome editing and mutant creation

CRISPR editing was used to mutate *CYP76M7* and *CYP76M8* genes. The CRISPR/Cas9 protocol has been described previously (Zhou *et al.*, 2014). Two guide RNA sequences targeting both *CYP76M7* and *CYP76M8* genes were designed, synthesised and used for the CRISPR/Cas9 construct, in order to mutate both genes simultaneously. Immature embryo-derived callus cells of rice (cv Kitaake) were transformed using the *Agrobacterium*

mediated rice transformation method. Transformed calli and regenerated plantlets were selected on medium containing hygromycin B. T0 lines were used for mutation screening, and T-DNA free homozygous mutant lines were selected in the corresponding T1 and T2 generation plants. The sequences of guide RNA and the corresponding primers used for mutation detection and plant genotyping are listed in Table S1.

Results

Hereditary stability of BGC deletions

To further investigate genetic stability of the BGC deletions the previously reported T0 lines (Zhou *et al.*, 2014) were selfed to generate T1 and T2 generations, with single plants homozygous for deletions of c2BGC or c4BGC and free from CRISPR constructs selected by PCR analysis. Specifically, for analysis of the c2BGC loci, one pair of primers, F1 and R1 flanking the 5' site (located at 21 662 kb of chr. 2), and another pair of primers, F2 and R2 flanking the 3' site (located at 21 906 kb of chr. 2), which were the locations of the sequences targeted for construction of this deletion, were designed (Fig. 1a; Table S1). PCR amplicons are only expected with the F1 and R1 or F2 and R2 primers from WT genomic DNA (gDNA), while amplicons with F1 and R2 were only expected from gDNA in which this region has been deleted (Figs 1a, S2a). Similarly, for analysis of the c4BGC, primer pairs F3 and R3, flanking the 5' site (located at 5323 kb of chr. 4) or F4 and R4, flanking the 3' site (located at 5485 kb of chr. 4) were used to detect the target sites used for this deletion, while F3 and R4 would only amplify gDNA with this *c.* 160 kb region deleted (Figs 1b, S2b; Table S1). Using these primers, individual plants were analysed during this selection process. The observed 1 : 2 : 1 segregation of WT, heterozygous and homozygous deletions (Fig. 1c,d; Table S2) indicated the hereditary stability of the large deletion mutations of both the c2BGC and c4BGC. For each BGC, a line homozygous for the deletion that was also CRISPR/Cas9 construct free (as verified by the lack of targeted PCR amplicons) was selected for further investigation; these are from this point forwards referred to as $\Delta c2bgc$ and $\Delta c4bgc$. Further analysis of these lines by RT-PCR indicated that the genes from the relevant (deleted) BGC were no longer expressed in these plants, consistent with their loss from the genome (Fig. S3a,b). The sequences of gene-specific oligonucleotides for expression are provided in Table S3.

A mutant line homozygous for deletion of both c2BGC and c4BGC was generated by crossing $\Delta c2bgc$ and $\Delta c4bgc$ mutant lines, with selection for homozygous loss of both BGCs via the same PCR-based approach as described previously (Fig. 1e). This line, with deletions of both c2BGC and c4BGC, is from this point forwards referred to as $\Delta c2/c4bgc$.

Effect of BGC deletions on LRD production

As it has been shown that rice production of LRDs can be induced by the application of copper chloride, enabling the detection of most of these natural products (Lu *et al.*, 2018),

investigation of such elicited leaf extracts was utilised here. In particular, to investigate how BGC deletion affected LRD production, leaves from the $\Delta c2bgc$, $\Delta c4bgc$ and $\Delta c2/c4bgc$ lines were induced and extracted, with analysis via an LC-MS method developed for this purpose (Lu *et al.*, 2018). Consistent with the multiple genes from the c2BGC associated with phytocassane biosynthesis (Fig. 1), these LRDs were no longer detectable from $\Delta c2bgc$ seedlings (Fig. 2a). By contrast, consistent with the remaining presence of the relevant *OsKSL10*, as well as *OsCPS1* (Fig. S1), production of oryzalexins A–F remained essentially unaffected (Fig. 2d). Conversely, consistent with the previously demonstrated importance of *CYP76M8* to momilactone biosynthesis (Kitaoka *et al.*, 2021), production of these LRDs was significantly reduced (Fig. 2b). Perhaps reflecting the increased availability of *syn*-CPP, production of the derived oryzalexin S was significantly increased (Fig. 2c). In $\Delta c4bgc$ plants, consistent with the multiple genes from this BGC associated with momilactone biosynthesis (Fig. 1), these LRDs were no longer detectable (Fig. 2b). Similarly, the *OsCPS4*-dependent (*syn*-CPP-derived) oryzalexin S also is essentially not produced (Fig. 2c). By contrast, production of phytocassanes was significantly increased (Fig. 2a), perhaps due to the increased availability of GGPP as has been speculated for *cps* mutants (Zhang *et al.*, 2021). Conversely, production of oryzalexins A–F was reduced (Fig. 2d). As expected, phytocassanes, momilactones and oryzalexin S were no longer detectable in $\Delta c2/c4bgc$ plants, and production of oryzalexins A–F was significantly reduced (Fig. 2a–d).

Effect on susceptibility to the fungal blast pathogen

Given the previously demonstrated differential effect of rice LRD phytoalexins on resistance to various species from the phytopathogenic fungal genus *Magnaporthe* and even strains of *M. oryzae* (Lu *et al.*, 2018), two *M. oryzae* strains (O254 and CA89) were examined here with $\Delta c2bgc$ and $\Delta c4bgc$ mutant plants as well as the parental/WT cv Kitaake. The O254 strain was from India, while CA89 was from California in the USA. Susceptibility was assayed by spray-inoculating rice seedlings at the three-leaf stage and analysing the diseased (discoloured) leaf area (Fig. 3). Consistent with the previous finding that the inducible *ent*-CPP-derived LRDs, which are largely dependent on *OsCPS2*, are effective phytoalexins against this pathogen (Lu *et al.*, 2018), $\Delta c2bgc$ and $\Delta c2/c4bgc$ mutant plants were significantly more susceptible to both strains, although this effect was much more pronounced with strain O254 than with CA89. By contrast, $\Delta c4bgc$ mutant plants did not exhibit significantly increased susceptibility to either strain of *M. oryzae* (Fig. 3a–d).

Effect on susceptibility to the bacterial leaf blight pathogen

It has previously been suggested that *OsCPS2*-dependent, *ent*-CPP-derived, but not *OsCPS4*-dependent (*syn*-CPP-derived), LRDs are effective against the rice bacterial leaf blight pathogen *Xoo* (Lu *et al.*, 2018; Zhang *et al.*, 2021). This was further examined here with $\Delta c2bgc$ and $\Delta c4bgc$ mutant plants compared with WT, using *Xoo* strain PXO99^A to infect 2-wk-old seedlings via

Fig. 2 Phytochemical profiling of $\Delta c2bgc$ and $\Delta c4bgc$ rice plants. (a–d) Effect of deleting the biosynthetic gene cluster from chromosome 2 (c2BGC) or the BGC from chromosome 4 (c4BGC) on labdane-related diterpenoid metabolism in rice relative to wild-type (WT) plants (average from three plants with error bars indicating standard deviation), specifically from analysis of leaves from 3-wk-old seedlings that were induced with CuCl_2 . **, $P < 0.01$; ***, $P < 0.001$; ns, no significant difference; calculated using post-ANOVA pairwise analysis of significance with the Dunnett's significant difference test for $\Delta c2bgc$, $\Delta c4bgc$ and $\Delta c2/c4bgc$ plants relative to the relevant WT line. Error bars represent \pm SD.

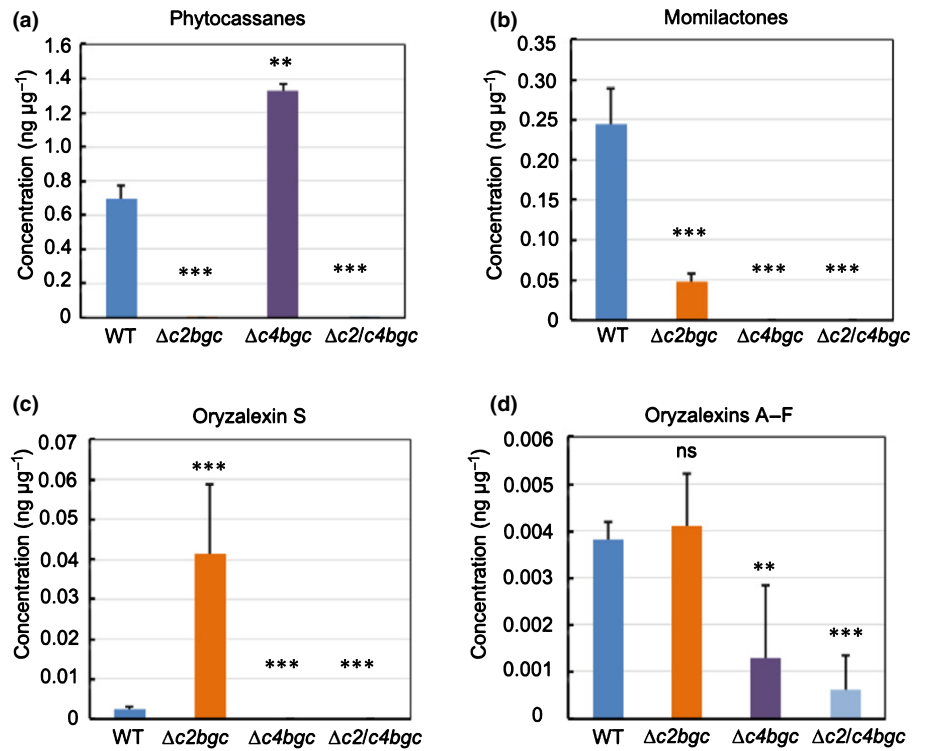
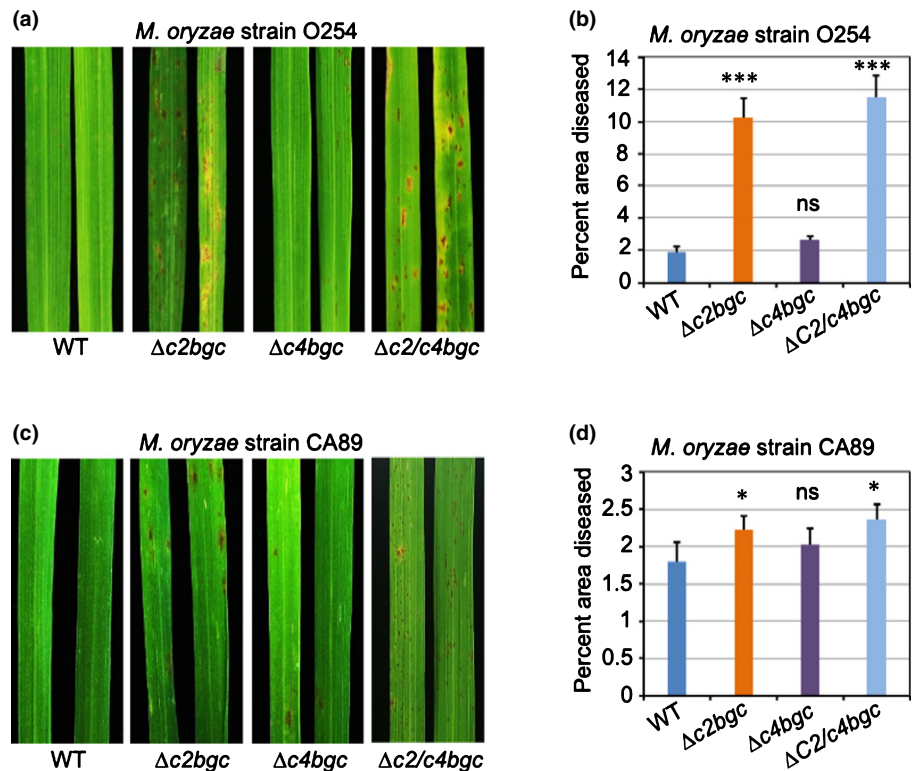


Fig. 3 Susceptibility of $\Delta c2bgc$, $\Delta c4bgc$ and $\Delta c2/c4bgc$ plants to *Magnaporthe oryzae*. (a, c) Representative leaves after infection with *M. oryzae* strains O254 (a) and CA89 (c) of rice plants at the three-leaf stage from the wild-type (WT), $\Delta c2bgc$, $\Delta c4bgc$ and $\Delta c2/c4bgc$ lines as indicated. (b, d) Percentage of diseased (discoloured) area vs total leaf area for $\Delta c2bgc$, $\Delta c4bgc$, $\Delta c2/c4bgc$ and WT plants after infection with *M. oryzae* strains O254 (b) and CA89 (d). *, $P < 0.05$; ***, $P < 0.001$; ns, no significant difference; calculated using post-ANOVA pairwise analysis of significance with Dunnett's significant difference test, for $\Delta c2bgc$ and $\Delta c4bgc$ plants relative to the relevant WT line. Error bars represent \pm SD.



infiltration and measuring bacterial numbers at 2 d post-infection (Fig. 4). As expected, $\Delta c2bgc$ and $\Delta c2/c4bgc$ plants were significantly more susceptible to *Xoo* (Fig. 4a), with almost a 10-

fold increase in colony forming units (CFU) relative to WT (Fig. b), while $\Delta c4bgc$ plants instead exhibited a slight but significant decrease in CFU (Fig. 4a,b).

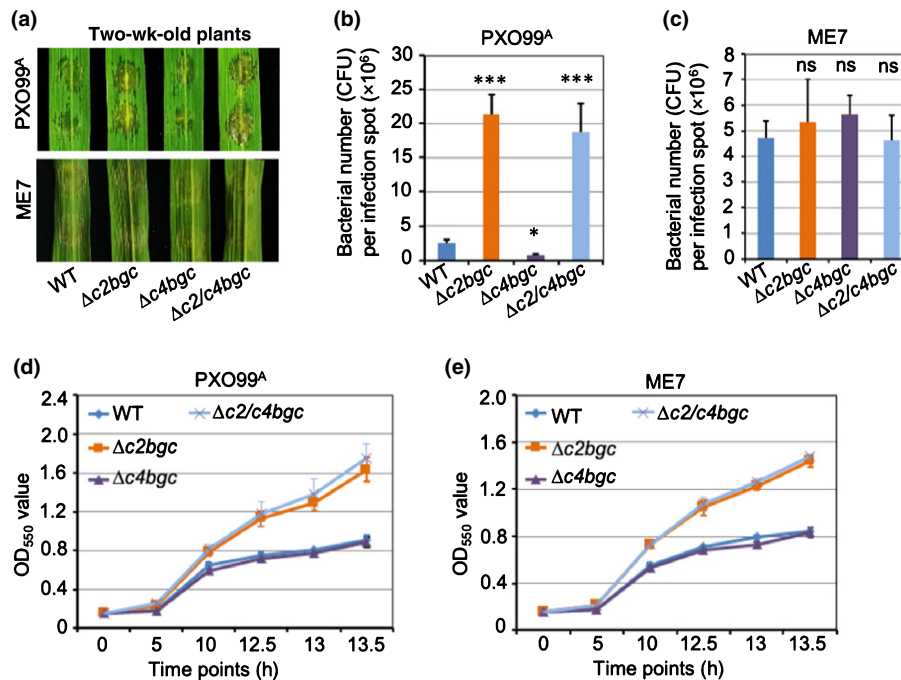


Fig. 4 *In vivo* and *in vitro* plant defence of $\Delta c2bgc$, $\Delta c4bgc$ and $\Delta c2/c4bgc$ rice plants against *Xanthomonas oryzae* pv. *oryzae* (*Xoo*). (a) Representative leaves from 2-wk-old plants of the wild-type (WT), $\Delta c2bgc$, $\Delta c4bgc$ and $\Delta c2/c4bgc$ lines after inoculation with *Xoo* strain PXO99^A (PXO99^A) (upper panel) or the type III secretion system, mutant PXO99^AME7 (ME7) strain (lower panel) via needless syringe infiltration. ME7 is incapable of type III effector secretion, is nonpathogenic and does not induce the microbial defence response in rice. (b, c) Susceptibility of WT, $\Delta c2bgc$, $\Delta c4bgc$ and $\Delta c2/c4bgc$ lines to infection with *Xoo* strain PXO99^A (b) or ME7 (c) measured by bacterial colony counting 2 d post-inoculation. *, $P < 0.05$; ***, $P < 0.001$; ns, no significant difference, calculated using post-ANOVA pairwise analysis of significance with Dunnett's significant difference test, for $\Delta c2bgc$, $\Delta c4bgc$ and $\Delta c2/c4bgc$ plants relative to WT. Error bars represent \pm SD. (d, e) Growth curves of PXO99^A (d) and its mutant ME7 (e) in medium containing root exudates from WT (control), $\Delta c2bgc$, $\Delta c4bgc$ and $\Delta c2/c4bgc$ mutant plants, as indicated. Error bars represent \pm SD.

c2BGC-dependent LRDs as phytoalexins and phytoanticipins against *Xoo*

The vast majority of rice LRDs are considered to be phytoalexins whose production is inducible (Peters, 2006), with accumulation of momilactones and phytocassanes specifically observed in *Xoo*-infected leaf tissues (Klein *et al.*, 2015). However, only the oryzalides and related (*ent*-isokaurene-derived) LRDs, whose production is not strongly inducible (Watanabe *et al.*, 1996), have been shown to exhibit antibiotic activity against *Xoo* and, hence, serve as phytoanticipins. The effectiveness of *ent*-CPP-derived (*O*₃CPS2-dependent) LRDs has been demonstrated by the increased susceptibility of *cps2* knock-out mutant plants to infection by *Xoo* (Lu *et al.*, 2018; Zhang *et al.*, 2021). However, it remains unclear if this effect was due to the activity of the relevant phytoanticipins (oryzalides and related LRDs) or phytoalexins (phytocassanes) against this bacterial phytopathogen. This was examined here with the *Xoo* mutant strain PXO99^AME7 (from this point forwards ME7), which is incapable of type III effector secretion and considered to be nonpathogenic, as it does not induce the plant defence response (Sugio *et al.*, 2007). Notably, ME7 grew at the same rate in the $\Delta c2bgc$, $\Delta c4bgc$ and $\Delta c2/c4bgc$ mutant plants relative to WT (Fig. 4a,c). To verify that the c2BGC-dependent LRDs still exhibited antimicrobial activity against the *Xoo* mutant strain ME7, as well as the parental pathogenic strain PXO99^A, bioassays were performed using root

exudates, which are known to contain some LRDs (Toyomasu *et al.*, 2008). In particular, root exudates from WT, $\Delta c2bgc$, $\Delta c4bgc$, and $\Delta c2/c4bgc$ seedlings were collected (separately) and was added to liquid culture medium, then used to grow PXO99^A and ME7 (again separately), with the growth rate observed by OD measurements (Fig. 4d,e). Consistent with general antibiotic activity of the c2BGC-dependent LRDs against *Xoo*, both PXO99^A and ME7 grew faster in medium with root exudates from $\Delta c2bgc$ and $\Delta c2/c4bgc$ mutant plants than with those from WT or $\Delta c4bgc$ mutant plants (Fig. 4d,e). The contrast between the unaffected growth of ME7 on $\Delta c2bgc$ mutant plants relative to the inhibitory effect of $\Delta c2bgc$ root exudates on ME7 growth in liquid culture indicated that rice produced c2BGC-dependent (*ent*-CPP-derived) LRDs as phytoalexins against *Xoo* in their leaves. In addition, given the effectiveness of such LRDs from uninduced root exudates against *Xoo* growth, it appears that these natural products also served as phytoanticipins in the rhizosphere.

A lesion mimic phenotype with $\Delta c2bgc$ plants

Consistent with the effect recently reported for *cps2* and *cps4*, as well as *cps2x4*, knock-out mutants in cv Kitaake (Zhang *et al.*, 2021), the $\Delta c2bgc$ and $\Delta c4bgc$ mutant plants exhibited a drought-sensitive phenotype (Fig. S4). Notably, the $\Delta c2bgc$, but not $\Delta c4bgc$ or $\Delta c2/c4bgc$, mutant plants were found also to

Fig. 5 Deletion of *c2BGC* leads to a lesion mimic (hypersensitive response) phenotype in rice. (a) Representative leaves from wild-type (WT), $\Delta c2bgc$, $\Delta c4bgc$ and $\Delta c2/c4bgc$ plants grown in a glasshouse (30°C) for 2 months after germination. (b) Representative leaves from WT and $\Delta c2bgc$ plants at the heading stage grown in a growth chamber at 23°C. (c) 3,3'-Diaminobenzidine (DAB) staining of the $\Delta c2bgc$ mutant and WT leaves before and after appearance of lesions (i.e. the indicated time after germination). (d–f) Relative expression level of defence-related genes *PBZ*, *PR1* and *POX22-3* in leaves from $\Delta c2bgc$, $\Delta c4bgc$ and $\Delta c2/c4bgc$ plants compared with WT. The leaf tissues were sampled before (6 wk) and after (8 wk) formation of lesions. Error bars represent \pm SD. (g) Representative leaves from WT and $\Delta c2bgc$ 8-wk-old plants infected with *Xanthomonas oryzae* pathovar *oryzae* (*Xoo*) (PXO99^A) via the leaf-tip clipping method to distinguish lesion length from lesion mimic spots. Arrowheads point to the edge of the infection progression. (h) Lesion length analysis for $\Delta c2bgc$ and WT plants after PXO99^A inoculation. ***, $P < 0.001$; calculated using post-ANOVA pairwise analysis of significance with Dunnett's significant difference test for $\Delta c2bgc$ plants relative to WT. Error bars represent \pm SD.

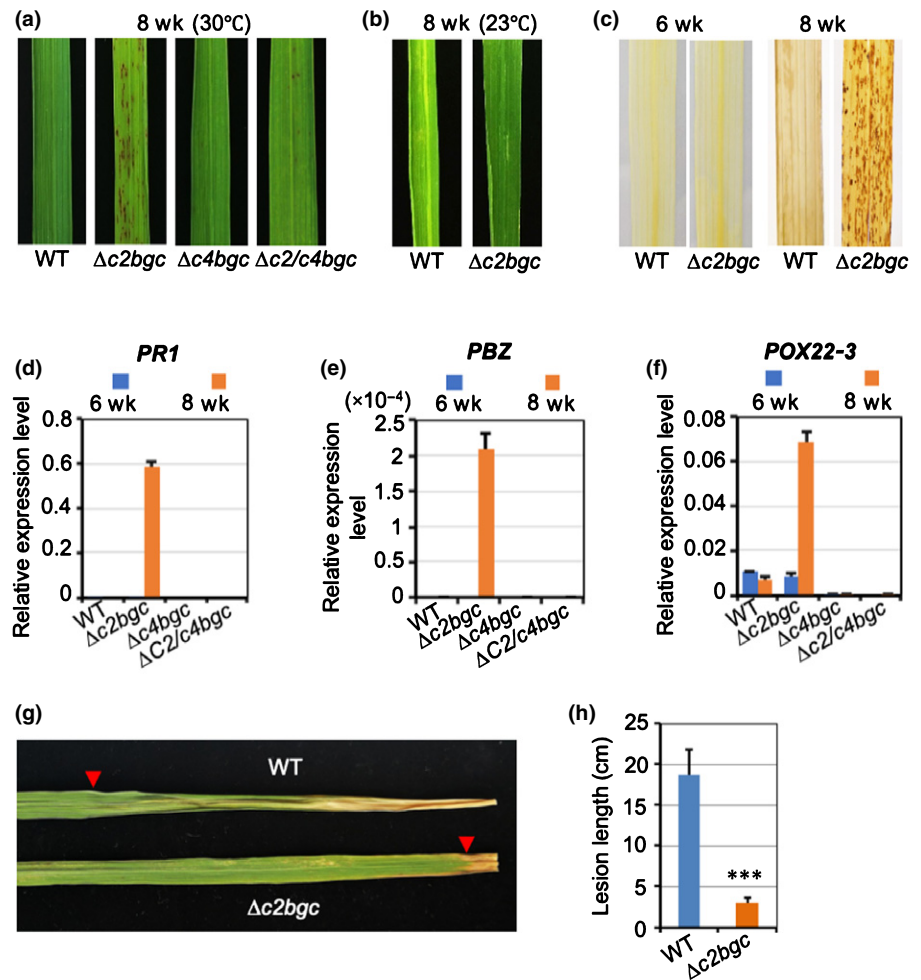


exhibit a lesion mimic phenotype *c.* 7 wk after germination, in the booting stage (Fig. 5a). This lesion mimic phenotype was temperature sensitive as, under low-temperature growth conditions (23°C), lesions were only rarely observed even in the heading stage of $\Delta c2bgc$ mutant plants (Fig. 5b).

To investigate the basis for lesion formation, leaves of the $\Delta c2bgc$ mutant plants were stained with DAB, with the observed formation of reddish-brown formazan precipitates indicative of H₂O₂ accumulation (Fig. 5c). Such reactive oxygen species can trigger either necrosis or programmed cell death (Van Breusegem & Dat, 2006), with the more specific hypersensitive response further coupled to defence responses (Balint-Kurti, 2019), which is often associated with lesion mimic mutants (Bruggeman *et al.*, 2015). Therefore, it was hypothesised that defence against pathogens in $\Delta c2bgc$ mutant plants might be enhanced. This was first investigated by analysis of the expression level of rice defence-related genes, including *PBZ* (Kim *et al.*, 2004), *PR1* (Mitsuhashi *et al.*, 2008) and inducible peroxidase *POX22-3* (Chittoor *et al.*, 1997), in $\Delta c2bgc$ leaves before and after lesion appearance. All the defence-related genes were significantly upregulated in $\Delta c2bgc$ mutant leaves with the appearance of the lesions, with no change in expression levels in $\Delta c4bgc$ and $\Delta c2/c4bgc$ mutant or WT plants during the same growth stage (Fig.

5d–f). Indeed, following lesion formation, the $\Delta c2bgc$ mutant plants exhibited enhanced resistance against *Xoo* PXO99^A relative to WT at the same growth stage (Fig. 5g,h). These results indicated that the lesion mimic phenotype exhibited by loss of the *c2BGC* arose from a hypersensitive response that appeared later in rice plant development.

CYP76M7 and *CYP76M8* are responsible for lesion mimic phenotype

To determine the gene(s) from the *c2BGC* responsible for the lesion mimic phenotype the relevant previously reported *cv* Kitaake mutant lines were examined – that is, *cps2* (Zhang *et al.*, 2021), as well as *cyp76m7* and *cyp76m8* (Kitaoka *et al.*, 2021). However, none of these single gene knock-outs exhibited this phenotype. Fortunately, it was recently noted that RNAi knock-down of the closely related paralogues *CYP76M7* and *CYP76M8* from the *c2BGC* led to a lesion mimic phenotype (Ye *et al.*, 2018). Therefore, a multiplex CRISPR/Cas9 approach was used to knock out both genes simultaneously (Fig. S5), with the resulting *cyp76m7/8* double-mutant plants found to exhibit the lesion mimic phenotype (Fig. 6a), as well as drought sensitivity (Fig. S6). As found for $\Delta c2bgc$ mutant plants, this lesion mimic

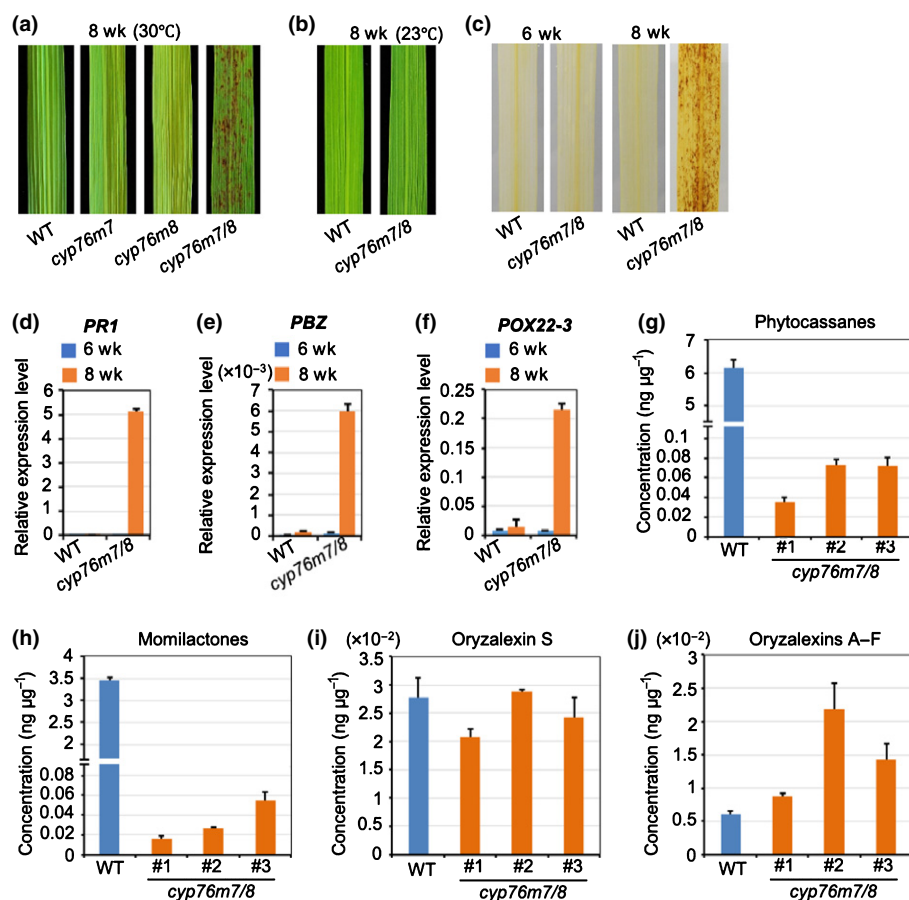


Fig. 6 Lesion mimic phenotypes and phytochemical profiling of rice double knock-out mutants of *cyp76m7* and *cyp76m8*. (a) Representative leaves of wild-type (WT), *cyp76m7*, *cyp76m8* and *cyp76m7/8* plants grown in a glasshouse (30°C) for 2 months after germination. (b) Representative leaves from the heading stage of WT and *cyp76m7/8* plants grown in a growth chamber at 23°C. (c) Diaminobenzidine (DAB) staining of *cyp76m7/8* and WT leaves before and after appearance of lesions. (d–f) Relative expression level of defence-related genes *PBZ*, *PR1* and *POX22-3* in leaves from *cyp76m7/8* plants compared with WT. The leaf tissues were sampled before (6 wk) and after (8 wk) formation of lesions. Error bars represent \pm SD. (g–j) Effect of *cyp76m7/8* double knock-out mutant on the labdane-related diterpenoid metabolism relative to WT plants. Error bars represent \pm SD.

phenotype was temperature sensitive, as under low-temperature growth conditions (23°C) lesions were similarly only rarely observed even in the heading stage (Fig. 6b). DAB staining of *cyp76m7/8* double-mutant leaves was observed to form reddish-brown formazan, indicating the accumulation of H_2O_2 (Fig. 6c). The expression level of rice defence-related genes, including *PBZ*, *PR1* and *POX22-3*, also was found to be markedly increased (Fig. 6d–f). Accordingly, the *cyp76m7/8* double mutant then seemed to be sufficient to induce the same hypersensitive response seen with $\Delta c2bgc$ plants.

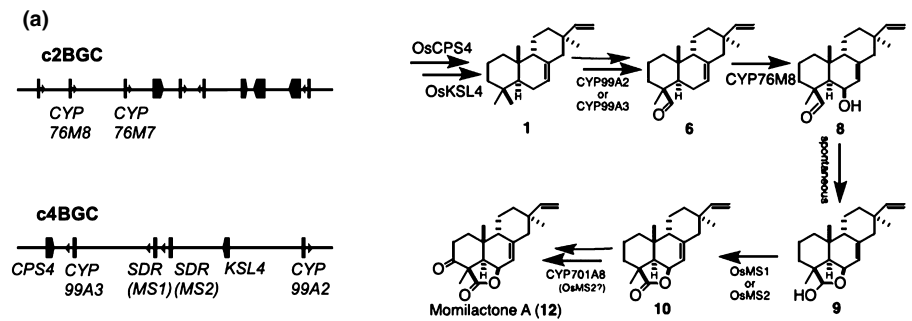
Investigation of secreted LRDs demonstrated that the *cyp76m7/8* double mutant exhibited significant reductions of both phytocassanes or momilactones, with no consistent effect on either oryzalexin S or oryzalexins A–F (Fig. 6g–j). Although both phytocassanes and momilactones were significantly reduced in *cyp76m7/8* double-mutant plants, the lesion mimic phenotype did not appear to be due to the reduction in LRD accumulation. In particular, despite similar reductions in these prevalent LRDs, the *cps2x4* (Zhang *et al.*, 2021) and $\Delta c2/c4bgc$ (Figs 5a, 7) double mutants did not display a lesion mimic phenotype. This contrast indicates that the LRDs are not simply acting as antioxidants, that is, to block accumulation of reactive oxygen species.

Discussion

While deletion of the two BGCs for LRD production in rice has been previously reported in heterozygous form (Zhou *et al.*,

2014), the results reported here demonstrated that this removal of substantial portions of the genome, and loss of associated biosynthetic capacity, is genetically stable. The effects of these deletion mutants on LRD production are consistent with the previously reported role of the *CYP76M* subfamily members (especially *CYP76M8*) from c2BGC in momilactone biosynthesis, which is alternatively associated with the c4BGC (Kitaoka *et al.*, 2021). The ability of $\Delta c2bgc$ mutant plants to produce some momilactones presumably is due to the previously reported ability of *CYP76M14*, located elsewhere in the genome, to catalyse the equivalent reaction (Kitaoka *et al.*, 2021). This contrasts with the essentially complete loss of momilactone production exhibited by the *cyp76m7/8* double-mutant lines, which may be explained by the inefficiency of the other *CYP76M* subfamily members in catalysing the relevant reaction. In particular, when only *CYP76M7* and *CYP76M8* are knocked out, rather than deletion of the whole c2BGC, other substrates with which the remaining *CYP76M* subfamily members exhibit greater catalytic efficiency may then be present, preventing these from acting in momilactone biosynthesis. Alternatively, this effect may be due to altered expression of these subfamily members in $\Delta c2bgc$ mutant plants relative to the *cyp76m7/8* double-mutant lines.

The effects of the two BGC deletion mutants on microbial disease resistance also was consistent with previously reported results (Lu *et al.*, 2018; Zhang *et al.*, 2021). However, the results from the *Xoo* bioassays reported here demonstrated that the c2BGC-dependent (*ent*-CPP-derived) LRDs exhibited direct antibiotic



Mutant	Phenotype (lesion mimic)	Conclusion
<i>cyp76m7</i>	No	<i>CYP76M7</i> and <i>CYP76M8</i> are redundant to each other. Lesion mimic should be due to intermediates or side-products in plants lacking <i>CYP76M7</i> and <i>CYP76M8</i> enzymes.
<i>cyp76m8</i>	No	
<i>cyp76m7/8</i>	Yes	
$\Delta c2bgc$	Yes	Products from c2BGC are not essential for lesion mimic.
$\Delta c4bgc$	No	
$\Delta c2/c4bgc$	No	Intermediates or side-products from c4BGC are essential for lesion mimic.
<i>cps4</i>	No	
<i>cps2/cps4</i>	No	

Fig. 7 Intermediates or side-products from the biosynthetic gene cluster from chromosome 4 (c4BGC) are genetically suggested to be reasons for lesion mimic in edited rice. (a) Genes from the BGC from chromosome 2 (c2BGC) (*CYP76M8*, plus *CYP76M7*) and c4BGC collaborate in the biosynthesis of momilactones. (b) Lesion mimic phenotype of single, double mutants and BGC deletion mutants, which suggests that intermediates or side-products from c4BGC are essential for lesion mimic. CYP, cytochrome P450; KSL, *ent*-kaurene synthase-like.

activity against this bacterial pathogen. Moreover, it is now also evident that these natural products serve as phytoalexins in the leaves as well as phytoanticipins in the rhizosphere. In addition, the c2BGC-dependent (*ent*-CPP-derived) LRDs exhibited differential effects on fungal blast resistance with the two strains of *M. oryzae* used here. Given that the LRD phytoalexins accumulated significantly faster in resistant, relative to susceptible, rice cultivars (Hasegawa *et al.*, 2010), it appears that the relevance of the LRD phytoalexins to the defence response depends on timely detection of the microbial pathogen by the rice host. Therefore, the differential results are presumably due to partial genetic (in)-compatibility between cv Kitaake rice and the *M. oryzae* strains used here, just as seen in other known plant–pathogen interactions (Delplace *et al.*, 2021).

The effect of the BGC deletion mutants on drought resistance again is consistent with previously reported results (Zhang *et al.*, 2021). In particular, the complete loss of either phytocassanes or momilactones, the most prevalent LRDs in rice, in $\Delta c2bgc$ and $\Delta c4bgc$ mutant plants (respectively), resembles the effect of the *cps2* and *cps4* knock-out mutants in which this phenotype was first observed. This supports the hypothesis that LRDs act as a regulatory switch, with accumulation above a certain threshold promoting stomatal closure (Zhang *et al.*, 2021). The *cyp76m7/8* double knock-out mutant lines, with significant reductions in both phytocassanes and momilactones, also exhibited this phenotype, again consistent with this hypothesis.

Perhaps most interesting is the observation of a lesion mimic phenotype with $\Delta c2bgc$ mutant plants. The results reported here indicated that this results from a hypersensitive response, which includes induction of the rice microbial defence response. Fortuitously, it was possible to dissect the c2BGC and identify the relevant genes for this phenotype as the closely related *CYP76M7* and *CYP76M8*. Intriguingly, despite exhibiting similar catalytic activity in recombinant settings, these are not redundant, with *CYP76M7* serving a more important role in phytocassane biosynthesis, while *CYP76M8* is more important for momilactone production (Kitaoka *et al.*, 2021). Nevertheless, only the *cyp76m7/8* double-mutant plants exhibited the lesion mimic phenotype.

It has been postulated that phytoalexins exhibit antioxidant activity, at least *in vitro* (Ahuja *et al.*, 2012), and the loss of such antioxidants would be consistent with the observed accumulation of H₂O₂ during the appearance of the lesion mimic phenotype. However, the lack of this phenotype in other mutant lines that exhibit analogous loss of LRD biosynthesis as $\Delta c2bgc$, most markedly $\Delta c2/c4bgc$, demonstrated that this is not simply due to antioxidant loss. Instead, the results suggested that phytotoxicity occurred in the absence of the c2BGC, particularly *CYP76M7* and *CYP76M8*, but required the presence of the c4BGC, leading to a hypersensitive response. Intriguingly, it has recently been shown that in *Nicotiana attenuata* knocking down the expression of CYPs involved in diterpenoid biosynthesis can lead to

accumulation of phytotoxic intermediates (Li *et al.*, 2021), and it seems likely that similar phytotoxic accumulation of LRD intermediates dependent on the c4BGC may occur in rice in the absence of *CYP76M7* and *CYP76M8* from the c2BGC. This is most likely to be due to intermediates from the c4BGC-associated momilactone biosynthesis, which has recently been elucidated (De La Pena & Sattely, 2021; Kitaoka *et al.*, 2021), particularly the *syn*-pimaradien-19-al substrate of *CYP76M8*. However, given the more general role of *O:CPS4* for all *syn*-CPP-derived LRDs in rice (not all of which are known; see Fig. S1), this requires further investigation.

Regardless of the underlying mechanism, the observed directional phytotoxicity between these two BGCs provides further insight into their evolution. While the role for such negative selection pressure in BGC assembly might suggest that *CYP76M7* and *CYP76M8* should have been 'recruited' from the c2BGC to c4BGC, this ignores their largely distinct biosynthetic roles and evolutionary history. In particular, an extensive phylogenomic comparison indicated that phytocassane biosynthesis and assembly of the associated c2BGC arose first, with momilactone biosynthesis with assembly of the associated c4BGC occurring later (Miyamoto *et al.*, 2016). Therefore, the *CYP76M* subfamily member originally recruited to the c2BGC must have been involved in phytocassane production, with subsequent gene duplication giving rise to a copy that became specialised for momilactone biosynthesis (*CYP76M8*). The interdependent evolution of these two BGCs has been previously noted (Kitaoka *et al.*, 2021). Nevertheless, the negative selection pressure (i.e. phytotoxicity) demonstrated here provides further insight into the constraints this has imposed. In particular, this evolutionary process seems to have been sufficient to alleviate the usual recruitment that might have otherwise been expected to move *CYP76M8* to the c4BGC. In any case, it is expected that further dissection of these intriguing genetic loci will provide additional insights into the underlying mechanisms, as well as evolutionary pressures for such BGC assembly.






Acknowledgements

This work was partially supported by the US Department of Agriculture – National Institute of Food and Agriculture (grant no. 2020-67013-32557 to RJP and BY) and the National Institutes of Health (grant no. GM131885 to RJB). The authors are grateful to the National Small Grain Collection for providing rice seed, to Bo Liu and Huanbin Zhou for initially generating the gene cluster deletion lines, and to Guo-Liang Wang for kindly providing the two strains of *M. oryzae*.

Author contributions

RL and JZ designed and performed experiments. ZL, RJP and BY conceived the project and obtained financial support. RL and JZ wrote the initial draft of the manuscript, RJP, ZL and BY revised the manuscript. RL and JZ contributed equally to this work.

ORCID

Riqing Li  <https://orcid.org/0000-0003-4397-2056>
Zhaohu Li  <https://orcid.org/0000-0002-3826-4373>
Reuben J. Peters  <https://orcid.org/0000-0003-4691-8477>
Bing Yang  <https://orcid.org/0000-0002-2293-3384>
Juan Zhang  <https://orcid.org/0000-0001-6337-4438>

Data availability

Data are available in the Supporting Information.

References

- Ahuja I, Kissen R, Bones AM. 2012. Phytoalexins in defense against pathogens. *Trends in Plant Science* 17: 73–90.
- Balint-Kurti P. 2019. The plant hypersensitive response: concepts, control and consequences. *Molecular Plant Pathology* 20: 1163–1178.
- Bi H, Yang B. 2017. Gene editing with TALEN and CRISPR/Cas in rice. *Progress in Molecular Biology and Translational Science* 149: 81–98.
- Bruggeman Q, Raynaud C, Benhamed M, Delarue M. 2015. To die or not to die? Lessons from lesion mimic mutants. *Frontiers in Plant Science* 6: 24.
- Cartwright DW, Langcake P, Pryce RJ, Leworthy DP, Ride JP. 1981. Isolation and characterization of two phytoalexins from rice as momilactones A and B. *Phytochemistry* 20: 535–537.
- Char SN, Li R, Yang B. 2019. CRISPR/Cas9 for mutagenesis in rice. *Methods in Molecular Biology* 1864: 279–293.
- Chittoor JM, Leach JE, White FF. 1997. Differential induction of a peroxidase gene family during infection of rice by *Xanthomonas oryzae* pv. *oryzae*. *Molecular Plant–Microbe Interactions* 10: 861–871.
- De La Pena R, Sattely ES. 2021. Rerouting plant terpene biosynthesis enables momilactone pathway elucidation. *Nature Chemical Biology* 17: 205–212.
- Delplace F, Huard-Chauveau C, Berthomé R, Roby D. 2021. Network organization of the plant immune system: from pathogen perception to robust defense induction. *The Plant Journal*. doi: 10.1111/tpj.15462.
- Goff SA, Ricke D, Lan TH, Presting G, Wang R, Dunn M, Glazebrook J, Sessions A, Oeller P, Varma H *et al.* 2002. A draft sequence of the rice genome (*Oryza sativa* L. ssp. *japonica*). *Science* 296: 92–100.
- Hasegawa M, Mitsuahara I, Seo S, Imai T, Koga J, Okada K, Yamane H, Ohashi Y. 2010. Phytoalexin accumulation in the interaction between rice and the blast fungus. *Molecular Plant–Microbe Interactions* 23: 1000–1011.
- Kauffman HE, Reddy APK, Hsieh SPY, Merca SD. 1973. An improved technique for evaluating resistance of rice varieties to *Xanthomonas oryzae*. *Plant Disease Reporter* 56: 537–541.
- Kim ST, Kim SG, Hwang DH, Kang SY, Kim HJ, Lee BH, Lee JJ, Kang KY. 2004. Proteomic analysis of pathogen-responsive proteins from rice leaves induced by rice blast fungus, *Magnaporthe grisea*. *Proteomics* 4: 3569–3578.
- Kitaoka N, Zhang J, Oyagbenro RK, Brown B, Wu Y, Yang B, Li Z, Peters RJ. 2021. Interdependent evolution of biosynthetic gene clusters for momilactone production in rice. *Plant Cell* 33: 290–305.
- Klein AT, Yagnik GB, Hohenstein JD, Ji Z, Zi J, Reichert MD, MacIntosh GC, Yang B, Peters RJ, Vela J *et al.* 2015. Investigation of the chemical interface in the soybean-aphid and rice-bacteria interactions using MALDI-Mass spectrometry imaging. *Analytical Chemistry* 87: 5294–5301.
- Li J, Halitschke R, Li D, Paetz C, Su H, Heiling S, Xu S, Baldwin IT. 2021. Controlled hydroxylations of diterpenoids allow for plant chemical defense without autotoxicity. *Science* 371: 255–260.
- Li R, Char SN, Yang B. 2019. Creating large chromosomal deletions in rice using CRISPR/Cas9. *Methods in Molecular Biology* 1917: 47–61.
- Lu X, Zhang J, Brown B, Li R, Rodriguez-Romero J, Berasategui A, Liu B, Xu M, Luo D, Pan Z *et al.* 2018. Inferring roles in defense from metabolic allocation of rice diterpenoids. *Plant Cell* 30: 1119–1131.
- Mitsuahara I, Iwai T, Seo S, Yanagawa Y, Kawahigasi H, Hirose S, Ohkawa Y, Ohashi Y. 2008. Characteristic expression of twelve rice *PRI* family genes in

- response to pathogen infection, wounding, and defense-related signal compounds (121/180). *Molecular Genetics and Genomics* 279: 415–427.
- Miyamoto K, Fujita M, Shenton MR, Akashi S, Sugawara C, Sakai A, Horie K, Hasegawa M, Kawaide H, Mitsuhashi W *et al.* 2016. Evolutionary trajectory of phytoalexin biosynthetic gene clusters in rice. *The Plant Journal* 87: 293–304.
- Murphy K, Zerbe P. 2020. Specialized diterpenoid metabolism in monocot crops: biosynthesis and chemical diversity. *Phytochemistry* 172: 112289.
- Muthayya S, Sugimoto JD, Montgomery S, Maberly GF. 2014. An overview of global rice production, supply, trade, and consumption. *Annals of the New York Academy of Sciences* 1324: 7–14.
- Nutzmann HW, Huang A, Osbourn A. 2016. Plant metabolic clusters – from genetics to genomics. *New Phytologist* 211: 771–789.
- Nutzmann HW, Scazzocchio C, Osbourn A. 2018. Metabolic gene clusters in eukaryotes. *Annual Review of Genetics* 52: 159–183.
- Peters RJ. 2006. Uncovering the complex metabolic network underlying diterpenoid phytoalexin biosynthesis in rice and other cereal crop plants. *Phytochemistry* 67: 2307–2317.
- Peters RJ. 2010. Two rings in them all: the labdane-related diterpenoids. *Natural Products Reports* 27: 1521–1530.
- Schmelz EA, Huffaker A, Sims JW, Christensen SA, Lu X, Okada K, Peters RJ. 2014. Biosynthesis, elicitation and roles of monocot terpenoid phytoalexins. *The Plant Journal* 79: 659–678.
- Sesma A, Osbourn AE. 2004. The rice leaf blast pathogen undergoes developmental processes typical of root-infecting fungi. *Nature* 431: 582–586.
- Shimura K, Okada A, Okada K, Jikumaru Y, Ko K-W, Toyomasu T, Sassa T, Hasegawa M, Kodama O, Shibuya N *et al.* 2007. Identification of a biosynthetic gene cluster in rice for momilactones. *Journal of Biological Chemistry* 282: 34013–34018.
- Sugio A, Yang B, Zhu T, White FF. 2007. Two type III effector genes of *Xanthomonas oryzae* pv. *oryzae* control the induction of the host genes *OsTFIIAgamma1* and *OsTFX1* during bacterial blight of rice. *Proceedings of the National Academy of Sciences, USA* 104: 10720–10725.
- Swaminathan S, Morrone D, Wang Q, Fulton DB, Peters RJ. 2009. CYP76M7 is an *ent*-cassadiene C11 α -hydroxylase defining a second multifunctional diterpenoid biosynthetic gene cluster in rice. *Plant Cell* 21: 3315–3325.
- Takos AM, Rook F. 2012. Why biosynthetic genes for chemical defense compounds cluster. *Trends in Plant Science* 17: 383–388.
- Toyomasu T, Kagahara T, Okada K, Koga J, Hasegawa M, Mitsuhashi W, Sassa T, Yamane H. 2008. Diterpene phytoalexins are biosynthesized in and exuded from the roots of rice seedlings. *Bioscience, Biotechnology, and Biochemistry* 72: 562–567.
- Toyomasu T, Usui M, Sugawara C, Otomo K, Hirose Y, Miyao A, Hirochika H, Okada K, Shimizu T, Koga J *et al.* 2014. Reverse-genetic approach to verify physiological roles of rice phytoalexins: characterization of a knockdown mutant of *OsCPS4* phytoalexin biosynthetic gene in rice. *Physiologia Plantarum* 150: 55–62.
- Tucker SL, Besi MI, Galhano R, Franceschetti M, Goetz S, Lenhert S, Osbourn A, Sesma A. 2010. Common genetic pathways regulate organ-specific infection-related development in the rice blast fungus. *Plant Cell* 22: 953–972.
- Van Breusegem F, Dat JF. 2006. Reactive oxygen species in plant cell death. *Plant Physiology* 141: 384–390.
- Wang Q, Hillwig ML, Okada K, Yamazaki K, Wu Y, Swaminathan S, Yamane H, Peters RJ. 2012. Characterization of CYP76M5–8 indicates metabolic plasticity within a plant biosynthetic gene cluster. *Journal of Biological Chemistry* 287: 6159–6168.
- Watanabe M, Kono Y, Esumi Y, Teraoka T, Hosokawa D, Suzuki Y, Sakurai A, Watanabe M. 1996. Studies on a quantitative analysis of oryzalides and oryzalic acids in rice plants by GC-SIM. *Bioscience, Biotechnology, and Biochemistry* 60: 1460–1463.
- Wu Y, Hillwig ML, Wang Q, Peters RJ. 2011. Parsing a multifunctional biosynthetic gene cluster from rice: biochemical characterization of CYP71Z6 & 7. *FEBS Letters* 585: 3446–3451.
- Xu M, Galhano R, Wiemann P, Bueno E, Tiernan M, Wu W, Chung IM, Gershenzon J, Tudzynski B, Sesma A *et al.* 2012. Genetic evidence for natural product-mediated plant–plant allelopathy in rice (*Oryza sativa*). *New Phytologist* 193: 570–575.
- Yamane H. 2013. Biosynthesis of phytoalexins and regulatory mechanisms of it in rice. *Bioscience, Biotechnology, and Biochemistry* 77: 1141–1148.
- Ye Z, Yamazaki K, Minoda H, Miyamoto K, Miyazaki S, Kawaide H, Yajima A, Nojiri H, Yamane H, Okada K. 2018. In planta functions of cytochrome P450 monooxygenase genes in the phytocassane biosynthetic gene cluster on rice chromosome 2. *Bioscience, Biotechnology, and Biochemistry* 82: 1021–1030.
- Yu J, Hu S, Wang J, Wong GK, Li S, Liu B, Deng Y, Dai L, Zhou Y, Zhang X *et al.* 2002. A draft sequence of the rice genome (*Oryza sativa* L. ssp. *indica*). *Science* 296: 79–92.
- Zhang J, Li R, Xu M, Hoffmann RI, Zhang Y, Liu B, Zhang M, Yang B, Li Z, Peters RJ. 2021. A (conditional) role for labdane-related diterpenoid natural products in rice stomatal closure. *New Phytologist* 230: 698–709.
- Zhou H, Liu B, Weeks DP, Spalding MH, Yang B. 2014. Large chromosomal deletions and heritable small genetic changes induced by CRISPR/Cas9 in rice. *Nucleic Acids Research* 42: 10903–10914.
- Zhu W, Yang B, Chittoor JM, Johnson LB, White FF. 1998. AvrXa10 contains an acidic transcriptional activation domain in the functionally conserved C terminus. *Molecular Plant–Microbe Interactions* 11: 824–832.
- Zi J, Mafu S, Peters RJ. 2014. To gibberellins and beyond! Surveying the evolution of (di)terpenoid metabolism. *Annual Review of Plant Biology* 65: 259–286.

Supporting Information

Additional Supporting Information may be found online in the Supporting Information section at the end of the article.

Fig. S1 Biosynthesis pathways of *ent*-CPP and *syn*-CPP-derived diterpenes and phytochemical analysis of oryzalexins.

Fig. S2 Genomic DNA sequence of $\Delta c2bgc$ and $\Delta c2bgc$ mutations.

Fig. S3 Relative expression level of biosynthetic genes from chromosome 2 and 4 gene clusters.

Fig. S4 Effect of $\Delta c2bgc$ and $\Delta c4bgc$ mutants on drought resistance.

Fig. S5 Mutations of *CYP76M7* and *CYP76M8* loci in *cyp76m7/8* double-mutant lines.

Fig. S6 Effect of *cyp76m7*, *cyp76m8* and *cyp76m7/8* mutations on drought resistance.

Table S1 Primers for mutation detection.

Table S2 Segregation of M_2 and F_2 populations.

Table S3 Primers for RT-PCR.

Please note: Wiley Blackwell are not responsible for the content or functionality of any Supporting Information supplied by the authors. Any queries (other than missing material) should be directed to the *New Phytologist* Central Office.